

Deformation and toughness of polymeric systems: 1. The concept of a critical thickness

M. C. M. van der Sanden*, H. E. H. Meijer and P. J. Lemstra

Centre for Polymers and Composites (CPC), Eindhoven University of Technology,

PO Box 513, 5600 MB Eindhoven, The Netherlands

(Received 15 June 1992)

A relationship between the macroscopic toughness, the intrinsic network (entanglement and/or crosslink) density and the relative thickness of polymeric systems, is presented. Toughness of amorphous, glassy polymers is mainly determined by the strain to break, since the yield stress generally only varies between 50 and 80 MPa. It was found that the strain to break strongly depends on the absolute thickness of the specimen or, equivalently, the local thickness within the (micro) structure of the material. Only below a certain critical thickness can the intrinsic strain at break of a polymer be reached. The absolute value of this critical thickness and the intrinsic strain at break of a polymer are both determined by the network density. In this paper polystyrene (PS), a polymer that is generally considered to be very brittle, was investigated with respect to the influence of absolute thickness on its strain to break. For thin isotropic tapes of PS it was demonstrated that this critical thickness is below 1 μm . Based on experiments with macroscopically 'thick' PS samples (3 mm), which are made locally thin by the introduction of small, non-adhering rubbery particles ('holes'), we could identify that the critical thickness is 0.05 μm for PS.

(Keywords: polystyrene; deformation; toughness; critical thickness; network density)

INTRODUCTION

The toughness of polymeric systems has been studied extensively in the past. The paramount factors governing fracture, deformation and ultimate ductility, however, are still a matter of debate¹⁻⁶. Toughness is determined by *extrinsic* variables such as sample dimensions, notch geometries, testing speed and temperature, and *intrinsic* parameters such as the molecular structure and microstructure or morphology of the specimen under investigation.

Recently, important contributions have been made towards a better understanding of the relationship between (ultimate) toughness and molecular structure, or microstructure, of polymer blends⁷⁻¹¹. In the case of glassy, amorphous polymers, the basic approach is that the entanglement network is retained upon quenching in the glassy state. The characteristics of the entanglement network, like the molecular weight between entanglements, M_e , can be estimated in the melt from the apparent rubber plateau modulus. Based on this analysis, one could distinguish between loosely and highly entangled glassy, amorphous polymers. Applying the classical concept of rubber elasticity, the maximum draw ratio of a network, λ_{max} , scales with $M_e^{1/2}$. Since the yield stress of glassy polymers only varies within the range of 50–80 MPa, the toughness, i.e. the work to break, is mainly determined by the strain at break of stretching the entanglement network to its maximum elongation. Following this simple analysis, which has been used before in drawing semicrystalline polymers in the solid state¹², one easily derives that polystyrene (PS) possesses a λ_{max} of ~ 4.2 (320%) and polycarbonate (PC) a λ_{max} of ~ 2.5 (150%).

In this perspective, PS is a more ductile than PC. In actual practice, however, one observes that PS is macroscopically brittle with a strain at break of less than 5%, whereas PC possesses a strain at break of approximately 100%, hence close to the theoretical limit. The premature fracture of PS is related to the uncontrolled crazing process. Upon deformation, crazing occurs locally, i.e. only the fibrils bridging the crazes are elongated. Donald and Kramer^{8,9} have shown that locally, inside a craze fibril or inside a plane stress deformation zone (λ_{craze} and λ_{DZ} , respectively), the extension ratio correlates very well with the theoretical value (λ_{max}).

A well known technique to control the local deformation mechanism is to add a second phase in the form of dispersed rubbery particles^{1,13}. An important parameter in these systems is the 'interparticle distance' (ID) as demonstrated by Wu and Borggreve^{10,11,14-16}.

In this paper, we present some results concerning the concept of a critical thickness below which brittle samples become ductile. PS is taken as the model system. Tapes consisting of alternating layers of PS and polyethylene (PE) were prepared in order to investigate the influence of the PS layer thickness on its tensile properties. The concept of a minimum thickness is also transformed to a standard (3 mm thick) PS system in which the critical thickness is achieved locally by introducing non-adhering rubbery particles, i.e. the equivalence of holes.

EXPERIMENTAL

Sample preparation

PS and PE were coextruded using a Multiflux static mixer^{17,18}, into thin laminated tapes of total thickness

*To whom correspondence should be addressed

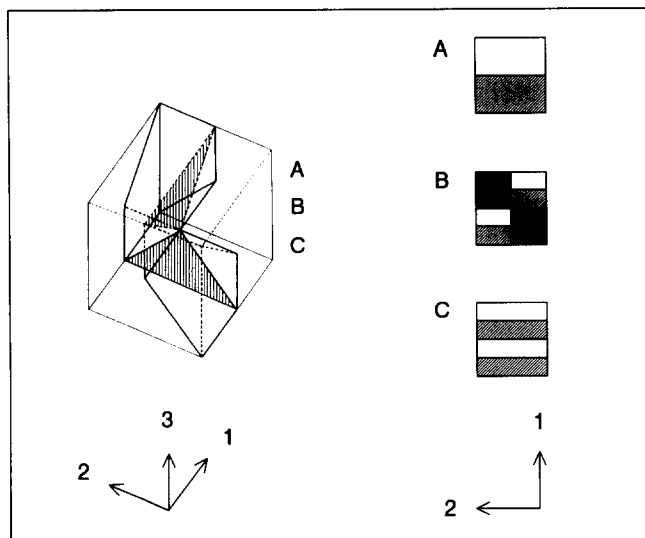


Figure 1 Principle of the Akzo Multiflux static mixer. One element is shown. In the text, 1 is referred to as the vertical direction, 2 the horizontal direction and 3 the direction of flow

around 0.3 mm, width 10 mm and infinite length, containing a varying number of layers (from eight up to 1024). PS and PE were used in five different proportions: PS/PE 100/0, 75/25, 50/50, 25/75 and 0/100. The principle of the static mixer is outlined in *Figure 1*. Starting with parallel layers of both polymers (stage A, *Figure 1*) the layers are split up and compressed vertically in opposite directions (stage B, *Figure 1*). Subsequently, an extension in the horizontal direction results in double the number of layers (stage C, *Figure 1*). If the number of elements is increased, so too is the total number of layers (power of two).

The extrusion temperature was 200°C and the total film thickness was kept constant (0.3 mm). The PS was of commercial grade (DOW, Styron 638) with a molecular weight of 70 kg mol⁻¹ and a polydispersity index of 2.85. The PE was a general purpose type supplied by DSM (LDPE 1808 AN). Small dumb-bell shaped tensile specimens were machined parallel to the direction of extrusion according to ASTM D 1708. In order to exclude any influence of orientation on the mechanical properties, the tapes were annealed at 80°C for at least 24 h.

Moulded PS samples, containing varying amounts of core-shell rubber (10–60 wt%) in order to obtain a small ligament thickness between the particles, were prepared in a co-rotating twin screw extruder (Werner and Pfleiderer ZSK 25) with a standard screw geometry, at an average barrel temperature of 125°C. In order to investigate the influence of adhesion between the rubbery particles and the matrix, on the tensile properties of rubber-modified PS, two different types of core-shell rubber were used: a non-adhering type I and an adhering type II. Type I core-shell rubber was a commercial grade supplied by Rohm and Haas Co. (Paraloid EXL 3647: styrene-butadiene core and a poly(methyl methacrylate) (PMMA) shell). The adhering rubbery particles (type II) consisted of a styrene-butadiene core and a PS shell, and were an experimental type of core-shell rubber kindly supplied by the General Electric Company. The size of the particles was in the range of 0.1–0.3 μm. Extruded strands were quenched, pelletized and subsequently injection moulded (Arburg Allrounder 220-75-250) into dumb-bell shaped tensile bars (DIN 53 455) at a

temperature of 200°C. In order to perform dilatometric measurements, a fraction of the pelletized materials was compression moulded into sheets, having a thickness of 3 mm. These sheets were machined into rectangular shaped specimens with a length of 100 mm and cross-sectional dimensions of 3 mm × 10 mm.

Mechanical testing

Before mechanical testing, both the injection-moulded and the compression-moulded tensile bars were annealed at 80°C for 24 h. Both the dumb-bell shaped layered samples of PS and PE and the dumb-bell shaped rubber-modified PS samples were strained at room temperature at a crosshead speed of 5 mm min⁻¹ on a Frank (type 81565 IV) tensile machine. Extensometers were used in the latter case to obtain accurate data concerning the stress-strain curves of the samples. At least five specimens were fractured for each blend composition.

The dilatometric experiments were performed on an Instron (type TTBM) tensile machine, equipped with a dilatometer filled with water. A detailed description of this method has been published elsewhere¹⁹, but some general aspects will be given here. Dilatometry allows measurement of the volume change ($\Delta V/V_0$) of the specimen during longitudinal straining. This is important with respect to the determination of the type of deformation mechanism occurring in the sample. If crazing occurs, this will be accompanied by an increase in volume (void formation) of the specimen during longitudinal elongation¹³. If, on the other hand, shearing is the main deformation mechanism, increasing the longitudinal strain will not result in an increase in volume strain. For rubber-modified materials it is not always clear whether a volume increase during straining is the consequence of dilatation of the rubbery particles, or the result of the crazing mechanism initiated at the rubbery particles. The strain rate applied in the dilatometer was 5 mm min⁻¹ and the span was 50 mm, resulting in a V_0 of 1500 mm³. The accuracy of the dilatometer was 1–2 mm³.

Scanning electron microscopy

Scanning electron microscopy (SEM, Cambridge Stereo Scan 200) was applied to investigate (i) the continuity and the thickness of the thin layers of PS and PE in the coextruded tapes, and (ii) the morphologies of the injection-moulded PS/rubber blends, to check the homogeneity of the distribution of the particles. In both cases, samples were cut parallel to the direction of extrusion at the centre of the specimen and subsequently sectioned at liquid nitrogen temperature with a glass knife, etched in an oxygen plasma and finally covered with a gold layer.

RESULTS AND DISCUSSION

The structure of multilayered tapes of PS/PE

Figure 2a is a SEM micrograph of an alternating PS/PE 50/50 w/w tape (three mixing elements), possessing both PS and PE layers of 10 μm thickness. It is clear from this micrograph that the adhesion between the PS and PE layers is poor, due to the fact that PE crystallizes (causing shrinkage) during cooling from the melt to room temperature. Consequently, PE serves as a perfect laminator for the thin stratified PS structures.

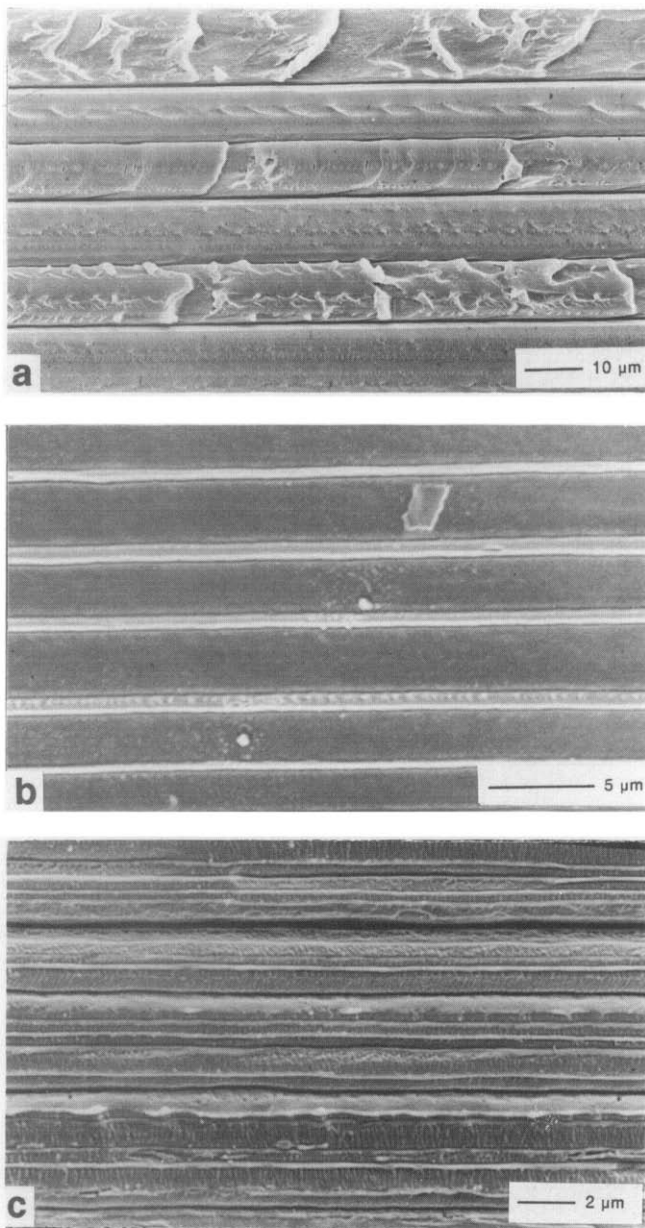


Figure 2 SEM micrographs of a PS/PE 50/50 w/w tape with three mixing elements (a); PS/PE 25/75 w/w tapes with six mixing elements (b) and nine mixing elements (c)

Figure 2b represents the minimum PS layer thickness attainable with this static mixing equipment: 0.8 μm (PS/PE 25/75 w/w; six mixing elements). Upon further increasing the number of elements, the tapes contain a lot of discontinuities due to rupture of the layers (Figure 2c: PS/PE 25/75 w/w; nine mixing elements).

The mechanical properties of PS tapes

Figure 3 shows the stress-strain curves of pure PS and PE tapes with a total tape thickness of about 0.3 mm. Curve A represents the typical stress-strain curve of PS: a breaking stress of 40 MPa and a strain at break of 1.5%. PE, on the other hand (Figure 3, curve B), is a very ductile polymer with a strain at break of about 225% under the same testing conditions.

In Figure 4, a stress-strain curve of a multilayered tape (PS/PE 25/75 w/w, six mixing elements) is shown. The sharp decrease in stress at 33% strain is the result of rupture of the PS layers. After passing this strong decrease

in stress the measurement is stopped, while the PE layers are unbroken, as indicated by the constant level of stress after passing 33% strain. If we assume that the stress-strain behaviour of PE is not influenced by a change in absolute thickness²⁰, we can (corresponding to the volume fraction of PE present in the total composite) subtract the stress-strain curve of PE from the stress-strain curve of the multilayered composite. The stress-strain trace of the thin PS component results.

In Figure 5, these traces are shown for four different tapes, with different PS/PE compositions and number of layers. Curve A corresponds to a PS layer thickness of 35 μm (PS/PE 50/50 w/w) and resembles the ordinary stress-strain behaviour of PS as observed in Figure 3, curve A. If the layer thickness of PS is decreased to 4.5 μm (PS/PE 25/75 w/w) the maximum stress is raised to 70 MPa and the strain at break is increased to a value of 5% (Figure 5, curve B). Further decreasing the PS layer thickness results in a shift of the strain at break to

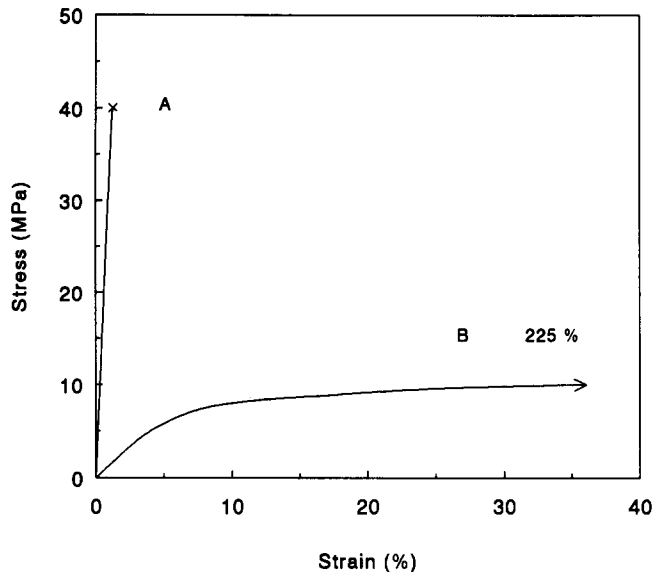


Figure 3 Stress-strain traces of the reference materials: A, PS; B, PE

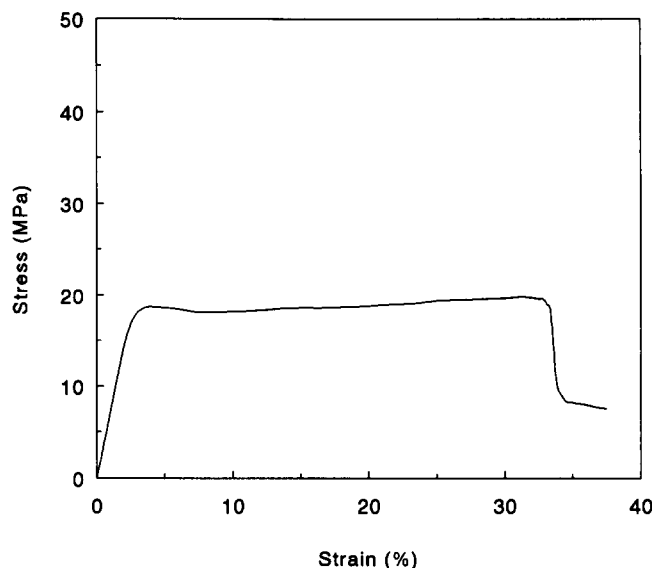


Figure 4 Stress-strain trace of a PS/PE 25/75 w/w multilayered tape (six mixing elements)

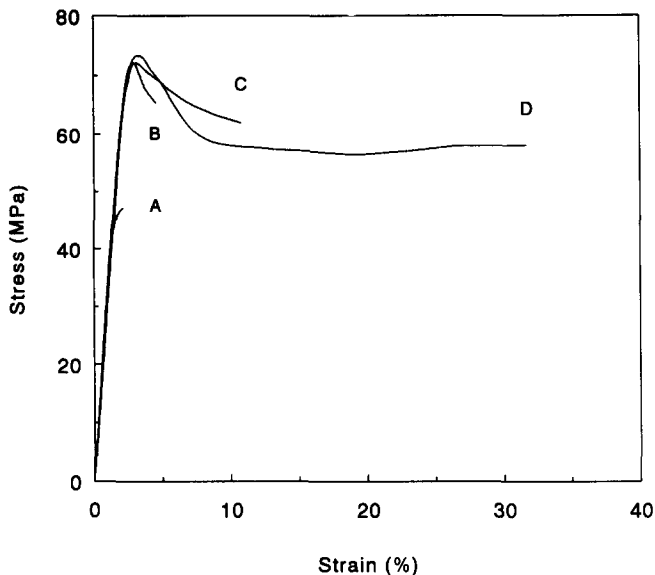


Figure 5 Stress-strain curves for pure PS tapes with varying PS layer thickness: A, 35 μm ; B, 4.5 μm ; C, 1.5 μm ; D, 0.8 μm

a value of more than 30% (Figure 5, curve D, thickness of PS layers is 0.8 μm ; PS/PE 25/75 w/w).

In Figure 6 the strain at break of PS is plotted as a function of the absolute PS layer thickness, as obtained from data of three different PS/PE ratios. As can be inferred from this figure, the 'critical thickness' for PS is below 1 μm for the given testing conditions. However, due to limitations in the minimum continuous PS layer thickness that could be achieved, the exact value of the critical PS layer thickness cannot be determined. Kramer and co-workers^{21,22} have also noticed a change in craze structure if the thickness of a PS film (free surface, exposed to air) was below 0.15 μm . Clearly, there is a close correspondence with the critical thickness of PS reported here.

A similar size effect in multilayered structures has been observed by Ma *et al.*²³. Their explanation for the strong increase in strain at break of multilayered composites upon decreasing the layer thickness, based on PC and styrene-acrylonitrile copolymer (SAN), was related to the micromechanics of these multilayered structures. In the PC/SAN system, analysed by Ma *et al.*, a considerable level of adhesion is present between the two constituents of the composite, while in the case of the PS/PE system the level of adhesion is negligible²⁴. Hence, the size effects observed in the non-adhesive PS/PE multilayered structures are probably not induced by complex micromechanics that depend strongly upon the precise level of adhesion.

In our PS/PE multilayered system, where adhesion is negligible, the explanation of an increase in drawability below a certain minimum thickness is straightforward. The process of deformation can only be sustained if the stress in the oriented parts is below the breaking stress, while the stress in the undeformed connected matrix surpasses the yield stress (analogous to the necking phenomenon in amorphous polymers²⁵). This principle can be generally applied to polymer systems provided that initiation of deformation always starts locally. By lowering the PS layer thickness (<1 μm) these conditions are approximated, resulting in a continuation of the process of deformation.

Rubber-modified PS

The principle of critical thickness, as approximated for thin layers of PS (<1 μm), should also exist in a standard PS sample if the local thickness inside the sample is below the critical value. In order to test this hypothesis, 'holes' were introduced to create multiple thin PS ligaments inside the material. Holes were generated by the introduction of rubbery particles, which should not be attached to the PS matrix. For this purpose core-shell rubbers were used, possessing a PMMA shell (type I): the PMMA does not adhere to the PS matrix²⁴ and, as a consequence of thermal shrinkage, the rubbery domains easily become detached from the PS matrix upon, or even before, mechanical deformation. In Figure 7 SEM micrographs of both types of core-shell rubber-modified PS samples are shown, containing different weight fractions of rubber (40, 50 and 60 wt%). The samples are cut from injection-moulded tensile bars parallel to the direction of extrusion. In all cases, discrete rubbery particles are observed without any significant agglomeration.

In Figure 8 the stress-strain curves of PS containing various amounts of type I core-shell rubber are shown (40, 50 and 60 wt%). Lower weight fractions of rubber are omitted for the sake of simplicity (these samples are all brittle, possessing a strain at break not exceeding 10%). Curve A corresponds to a blend containing 40 wt% core-shell rubber. The strain to break is rather low if the high weight fraction of rubber is considered. Increasing the rubber weight fraction to 50 wt% results in an increase in strain to break to 25%, comparable with the strain to break of commercially available high impact polystyrene, containing a rubber weight fraction of only about 25%, but with a different microstructure. However, upon adding 60 wt% core-shell rubber a sharp increase in strain to break is observed, clearly related to this

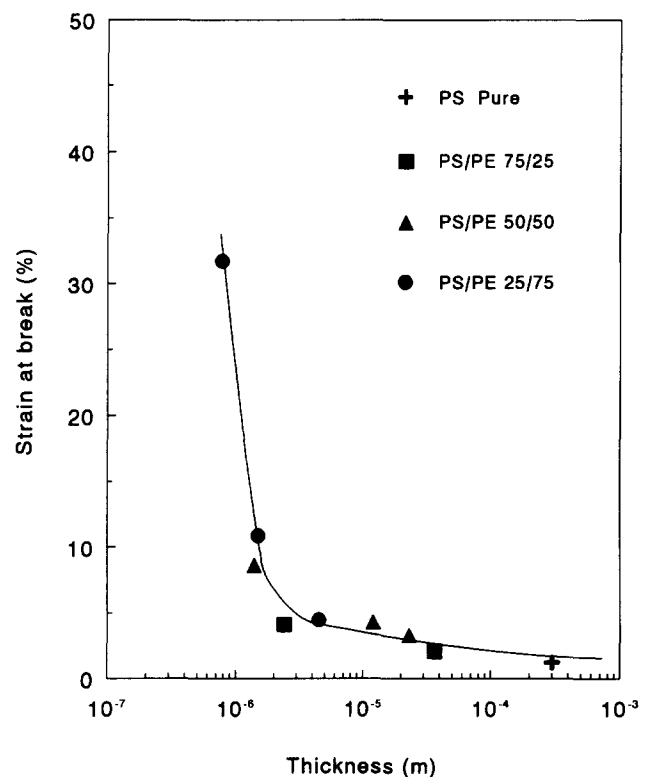


Figure 6 Strain at break of PS tapes as a function of PS layer thickness

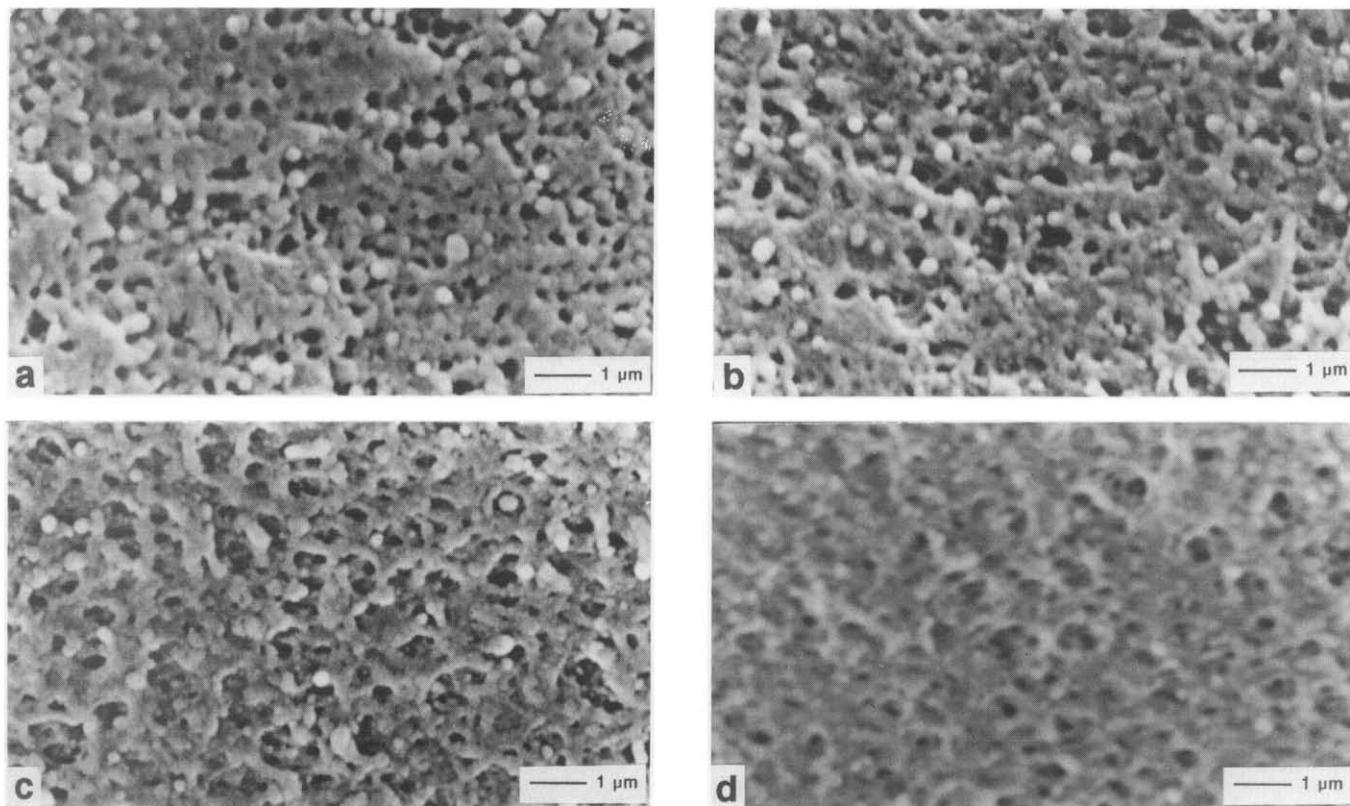


Figure 7 SEM micrographs of core-shell rubber-modified PS: (a) 40 wt% type I; (b) 50 wt% type I; (c) 60 wt% type I; (d) 60 wt% type II

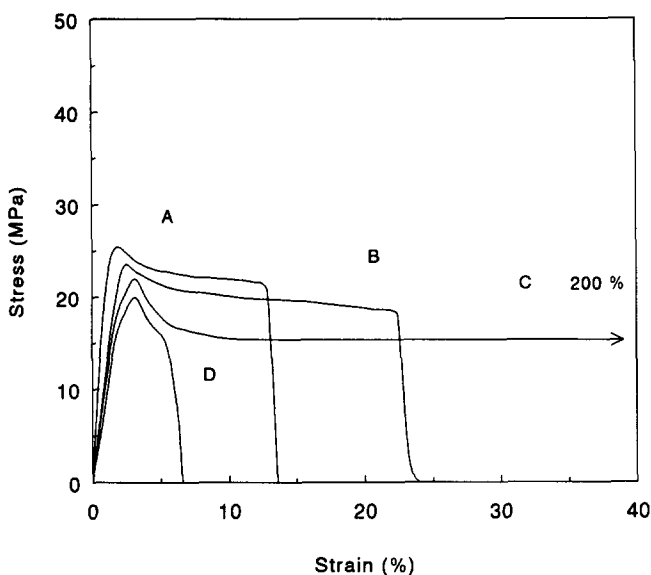


Figure 8 Stress-strain curves of type I core-shell rubber-modified PS (A, 40 wt%; B, 50 wt%; C, 60 wt% rubber) and type II core-shell rubber-modified PS (D, 60 wt% rubber)

critical ligament thickness below which a sharp increase in ductility is obtained. Clearly, local deformation can be initiated at stress concentrations near defects ('holes') and more or less controlled by the introduction of a second, low modulus phase; however, deformation, i.e. stretching of the entanglement network, can only be sustained if the sample as a whole follows this deformation process. If the average distance between the rubber particles is calculated¹⁶ (ID) (due to the high rubber volume fraction a body-centred lattice is assumed) it can be stated that the critical interparticle distance (ID_c)

for PS is located at $0.05 \mu\text{m}$. The PS modified with 50 wt% rubber contains ligaments of a thickness of about $0.06 \mu\text{m}$, which is clearly above the critical thickness, while the 60 wt% rubber-modified sample contains matrix ligaments of a thickness of about $0.04 \mu\text{m}$, which is obviously just below the critical ligament thickness.

To check the importance of the absence of adhesion in obtaining locally thin PS ligaments which can easily be stretched to a macroscopic strain of 200%, core-shell rubbers were also applied having a polystyrene shell (type II; perfect adhesion to the PS matrix). Even if 60 wt% of the adhering core-shell rubber is present in the PS matrix, only a strain at break of about 6% is measured (Figure 8, curve D).

To gain more insight into the type of deformation mechanism of blends containing PS and the non-adhering (type I) core-shell rubber, tensile tests have been performed with simultaneous volume measurements. Figure 9 shows the results of these measurements for PS blends containing 40 wt% (curve A), 50 wt% (curve B) and 60 wt% (curve C) type I core-shell rubber (the volume-strain curves for the blends containing 10, 20 and 30 wt% rubber are omitted for the sake of simplicity). For the blend containing 40 wt% core-shell rubber, the ($\Delta V/V_0$) curve increases slightly in the region of elastic behaviour (0–1.5% longitudinal strain). At a longitudinal strain of about 2.5% the slope of the curve increases sharply. This may result from either of two processes: (1) the core-shell rubber becomes more detached from the PS matrix; or (2) the crazing mechanism is operative in this material¹³. The slope of the volume-strain curve goes asymptotically to unity, indicating an equilibrium between the increase in volume strain (void content) and the increase in elongational strain. If the rubber concentration is increased to 50 wt%, almost the same

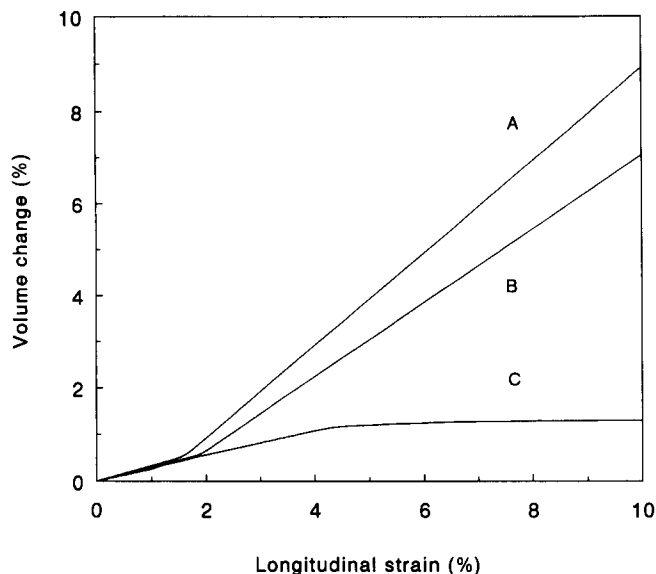


Figure 9 Volume-strain curves of type I core-shell rubber-modified PS: A, 40 wt%; B, 50 wt%; C, 60 wt% rubber

behaviour is observed for the volume-strain curve, except that in this case the slope of the curve is less than unity, after passing the elastic region. This implies that the increase in void content is lower than the increase in longitudinal elongation. This can only be explained by a contribution of shear deformation to the total deformation behaviour of the sample¹³, since it is known that the mechanism of shear deformation occurs without an increase in sample volume. Finally, curve C clearly confirms this statement: in this case the slope of the ($\Delta V/V_0$) curve decreases to zero and remains at zero until the maximum strain of 200% is reached, indicating that under these conditions the sample deforms purely by shear deformation. Hence, a transition from crazing to shear deformation occurs if the interparticle distance is decreased from $0.06 \mu\text{m}$ (50 wt% rubber) to $0.04 \mu\text{m}$ (60 wt% rubber), which correlates well with the sharp increase in strain to break, shown in Figure 8.

The value of ID_c obtained for type I core-shell rubber-modified PS is more accurate than the value obtained from the multilayer composites. This is due to the limitations in PS layer thickness obtainable for the PS/PE system. At a layer thickness of $0.8 \mu\text{m}$, only the onset of a sharp increase of the strain to break is measured and the critical layer thickness is obviously not yet reached. A further reduction of layer thickness should lead to a strain to break comparable with the value obtained with type I core-shell rubber-modified PS (200%). Additional experiments with a newly designed multilayer mixer revealed that, if the viscosities of the two polymers are closely matched such as for the model system PS/PMMA, the minimum thickness of still continuous layers, can be reduced to 80 nm. However, for the system PS/PE these low values could not be reached.

CONCLUSIONS

Local thickness

It was shown that brittle polymers become ductile below a critical thickness, as demonstrated for isotropic tapes of PS. The onset of a sharp increase in strain to

break of PS was found if the thickness was reduced below $1 \mu\text{m}$. The exact value of the critical thickness could not be determined using layered structures, because the minimum continuous PS layer thickness that could be achieved was restricted to $0.8 \mu\text{m}$. The true yield stress of PS was found to be about 70 MPa.

For rubber-modified PS, the influence of the local ligament thicknesses on the mechanical response was investigated, and the exact value of the critical surface-to-surface interparticle distance (i.e. ligament thickness) was determined to be $0.05 \mu\text{m}$. Below this critical value the material demonstrates a remarkable ductile behaviour.

Influence of network density

Our research is aimed at an overall investigation of the ultimate toughness of polymeric systems, by varying systematically the intrinsic network (entanglement and/or crosslink) density and the local thickness of the system (see Figure 10). The drawn line in Figure 10 corresponds to the theoretical strain at break based on the intrinsic network structure (λ_{max}). For PC the macroscopic strain at break is close to the theoretical value (Figure 10, filled circle). For PS, however, the macroscopic strain at break of a standard sample (Figure 10, open square), is far below the theoretical value. However, if the (local) thickness of PS is below its critical value, the macroscopic strain at break (Figure 10, filled square) approximates the expected value rather well (as shown in this paper).

In two subsequent papers^{26,27} the critical (ligament) thickness between non-adhering (or cavitated) rubbery particles will be investigated for other polymer systems, with different network density. In particular, the relationship between the absolute value of this critical thickness and the intrinsic molecular network structure will be emphasized. In part 2²⁶, entangled structures will be dealt with using the model system PS/poly(2,6-dimethyl-1,4-phenylene ether) in order to set the entanglement density. Part 3²⁷ will focus on different thermoset systems which can be considered as rather 'densely' crosslinked structures in terms of network density, compared with thermoplastic polymers.

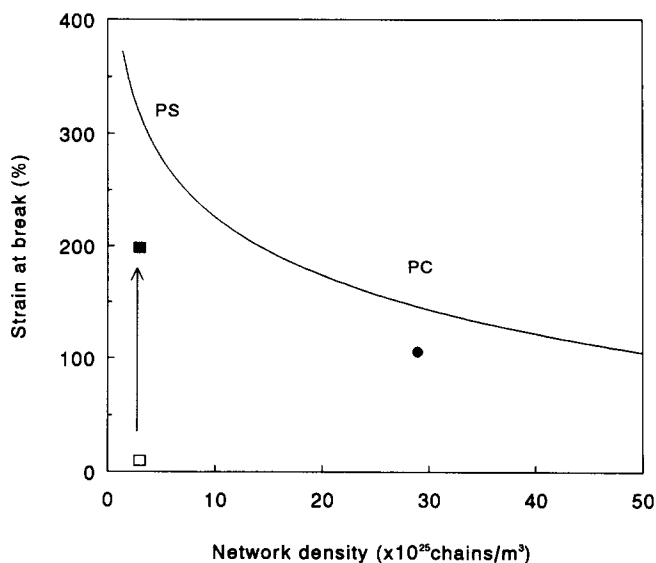


Figure 10 Strain at break versus network (entanglement and/or crosslink) density. The drawn line represents the theoretical strain at break of the polymer network. See text for details

ACKNOWLEDGEMENTS

The authors are grateful to A. E. P. van Etten for carrying out the experiments on the layered structures and to J. J. Crevecoeur for performing the mechanical analysis of the various rubber-modified polystyrene blends. This work was supported by the Foundation for Polymer Blends (SPB).

REFERENCES

- 1 Bucknall, C. B. 'Toughened Plastics', Applied Science Publishers, London, 1977
- 2 De Gennes, P. G. *Europhys. Lett.* 1991, **15** (2), 191
- 3 Parker, D. S., Sue, H. J., Huang, J. and Yee, A. F. *Polymer* 1990, **31**, 2267
- 4 Brown, H. R. *Macromolecules* 1991, **24**, 2752
- 5 Termonia, T. and Walsh, D. J. *J. Mater. Sci.* 1989, **24**, 247
- 6 Michler, G. H. *J. Mater. Sci.* 1990, **25**, 2321
- 7 Kramer, E. J. and Berger, L. L. *Adv. Polym. Sci.* 1990, **91/92**, 1
- 8 Donald, A. M. and Kramer, E. J. *Polymer* 1982, **23**, 461
- 9 Donald, A. M. and Kramer, E. J. *Polymer* 1982, **23**, 1183
- 10 Wu, S. *Polym. Eng. Sci.* 1990, **30** (13), 753
- 11 Wu, S. *Polymer* 1985, **26**, 1855
- 12 Smith, P., Lemstra, P. J., Kalb, B. and Pennings, A. J. *Polym. Bull.* 1979, **1**, 733
- 13 Kinloch, A. J. and Young, R. J. 'Fracture Behaviour of Polymers', Elsevier, London, 1985
- 14 Borggreve, R. J. M., Gaymans, R. J., Schuijjer, J. and Ingen Housz, J. F. *Polymer* 1987, **28**, 1489
- 15 Borggreve, R. J. M. PhD Thesis, Twente University of Technology, The Netherlands, 1988
- 16 Wu, S. *J. Appl. Polym. Sci.* 1988, **35**, 549
- 17 Sluijters, R. *De Ingenieur* 1965, **77** (15), 33
- 18 Schilo, D. and Ostertag, K. *Verfahrenstechnik* 1972, **6** (2), 45
- 19 Coumans, W. J. and Heikens, D. *Polymer* 1980, **21**, 957
- 20 Pan, S. J., Hill, M. J., Keller, A., Hiltner, A. and Baer, E. *J. Polym. Sci., Polym. Phys. Edn* 1990, **28**, 1105
- 21 Donald, A. M., Chan, T. and Kramer, E. J. *J. Mater. Sci.* 1981, **16**, 669
- 22 Chan, T., Donald, A. M. and Kramer, E. J. *J. Mater. Sci.* 1981, **16**, 676
- 23 Ma, M., Vijayan, K., Hiltner, A., Baer, E. and Im, J. *J. Mater. Sci.* 1990, **25**, 2039
- 24 Wu, S. 'Polymer Interface and Adhesion', Dekker, Basel, 1982
- 25 Ward, I. M. 'Mechanical Properties of Solid Polymers', Wiley-Interscience, London, 1971, p. 274
- 26 Van der Sanden, M. C. M., Meijer, H. E. H. and Lemstra, P. J. *Polymer* in press
- 27 Van der Sanden, M. C. M., Meijer, H. E. H. and Lemstra, P. J. *Polymer* submitted